Quang Khanh Nguyen[1], Le Hung Trinh[2*], Khanh Hoai Dao[2], Nhu Duan Dang[3]

[1] Hanoi University of Mining and Geology, North Tuliem District, Hanoi, Vietnam
[2] Le Quy Don Technical University, Hoang Quoc Viet Street, Hanoi, Vietnam
[3] Vietnam Institute of Geodesy and Cartography, Hoang Quoc Viet Street, Hanoi, Vietnam
*Corresponding author: trinhlehung125@gmail.com

LAND SURFACE TEMPERATURE DYNAMICS IN DRY SEASON 2015-2016 ACCORDING TO LANDSAT 8 DATA IN THE SOUTH-EAST REGION OF VIETNAM

ABSTRACT. Located in Southeast Asia, Vietnam is one of the most severely affected countries by climate change and faces to series of challenges related to climate change, in which droughts are one of the most serious natural disasters. Land surface temperature (LST) is important factor in evaluating soil moisture and drought phenomenon. Remote sensing technique with many advantages, compared with traditional methods, can be used effectively for retrieving LST. This article presents study on the application of LANDSAT 8 multi – temporal data for monitoring LST changes in dry season 2015 – 2016 in Loc Ninh district, Binh Phuoc province in Southeast region of Vietnam. LST was derived using Split-Window (SW) algorithm. The results showed that the LST at the end of 2015 – 2016 dry seasons (in February and March) is much higher than at the early of dry season. The area with LST higher than 309 K increases very fast in dry season 2015 – 2016, from less than 1% of the total study area in November and December to 19.59% in February and 30.74% in March. The results obtained in this study can be used to create the LST distribution map and to monitor drought phenomenon.

KEY WORDS: remote sensing, LST, drought, thermal infrared, LANDSAT, Vietnam

INTRODUCTION

Vietnam is likely to be one of the several countries most adversely affected by climate change. During the last 50 years, Vietnam's annual average surface temperature has increased by approximately 0.5 – 0.7 0C (Vietnam assessment report on climate change). LST is important fac-tor in global change studies, in estimating radiation budgets in heat balance studies and as a control for climate models. LST can provide important information about the surface physical properties and climate which plays a role in many environmental processes (Mallick et al. 2008; Mira 2007). The estimation of LST pays important role in numerical modeling especially in phys-

ical based hydrological models where water balance/budgeting of the catchment is an important component (Thakur and Gosavi 2018).

Many researchers have used remote sensing data to determine and monitor LST distribution. Retrieval of LST using thermal infrared bands of satellite images is the most effective way to derive energy balance and evapotranspiration (ET) on regional basis (Pariada et al. 2008). Since the last of 20th century, satellite-derived surface temperature data have been utilized for regional climate analyses on different scale (Carnahan and Larson 1990). Beginning with Landsat 4, Landsat satellite series provides the data for retrieval of LST for longer period of time. Landsat 5 TM and Landsat 7 ETM+ data were used to estimate LST in urban area (Alipour et al. 2007; Mallick et al. 2008; Kurma et al. 2012; Balling and Brazel 1988; Grishchenko 2012; Marchokov and Trinh 2013; Tran et al. 2009; Trinh 2014). The results of these studies have demonstrated that in the big cities, urban heat island effect is becoming a problem due to increasing coverage of land with asphalt pavements.

The relationship between LST and vegetated areas has been documented in the many studies. Cueto et al. (2007) found correlation between surface temperature in Mexicali (Mexico) and land use by using remote sensing data. Hyung Moo Kim et al. (2005) proposed algorithm to estimate the statistical correlation between LST and vegetation index. A study by Cai et al. (2017) analyzed the relationship between LST and land cover changes in Zhengzhou city (Huabei Plain) using multi-temporal satellite data. They examined the usefulness of Landsat 5 TM imagery for classifying land cover/land use and using thermal infrared band (band 6) to produce a thermal map of Zhengzhou city.

LST is also one of the most important factors in studying drought phenomenon, as well as input parameters for climate models (Alshaikh 2015). Many studies have proven that a combination of surface temperature and normalized difference vegetation in-

dex (NDVI) can provide information about surface soil moisture. A study by Lambin and Ehrlich (1996) reviewed extensively the drivers between normalized difference vegetation index (NDVI) and brightness temperature (BT), and described a general spatial pattern of relationships between NDVI and BT, related to land cover. They concluded that BT/NDVI slope could be used to classify land cover, and monitor land cover changes over time when associated to seasonality information, retrieved from NDVI annual variations alone (Julien and Sobrino 2009). Sandholt et al. (2002) proposed a drought index called Temperature Vegetation Dryness Index (TVDI), which is calculated from satellite derived vegetation index (NDVI) and surface temperature. This drought index is also used in many other studies to assess soil moisture and drought status (Zverev and Trinh 2015; Chen et al. 2011; Shang et al. 2017).

A number of algorithms have been used to estimate the LST using remote sensing thermal infrared (TIR) data as it is capable to decipher the thermal characteristic of the land surface. These algorithms are namely mono-window (MW), split-window (SW), dual-angle (DA), single-channel (SC)… (Galve et al. 2008; Rongali et al. 2018). The studies carried out in different areas, such as the northern Negev Desert, Israel (Du et al. 2014; Rozenstein et al. 2014) and the Beas River basin, India (Rongali et al., 2018) show that the split-window algorithm can be adjusted for estimating LST from Landsat 8 data to get better accuracy. The objective of our paper is to evaluate the dynamics of LST in Loc Ninh district, Binh Phuoc province of Southeast region of Vietnam during 2015 – 2016 dry season using Landsat 8 multi-temporal data. SW algorithm was used to calculate LST from Landsat 8 data in this case study.

STUDY AREA AND MATERIALS

Loc Ninh is a mountainous district in the northwestern border of Binh Phuoc province, with a borderline of over 100 kilometers. It is bordered by Kratie and Cong Pong Cham provinces (Cambodia). The area is bounded between latitude $11^0 39'6.09''N$ to

12⁰05'50.7"N and longitude 106⁰24'39.5"E to 106⁰59'19.3"E (Fig. 1) (locninh.binhphuoc.gov.vn, 2018). The district covers an area of 853.95 km² and had a population of 115268 people (locninh.binhphuoc.gov.vn, 2018). Loc Ninh district has a high terrain in the north and low terrain in the south. It located in tropical monsoon region; the climate is divided into two seasons: the rainy season from May until October and the dry season from November to April, while March and April are the warmest and driest months. This is the largest pepper growing area of Binh Phuoc province and also is one of the most regions severely affected by drought in Southeast region of Vietnam.

In this study, five multispectral cloud – free LANDSAT 8 OLI - TIRS images (path 124,

row 52) with a spatial resolution of 30x30 meters were acquired from November 24, 2015, December 26, 2015, January 11, 2016, February 28, 2016 and March 31, 2016 (Fig. 2). The LANDSAT 8 data was the standard terrain correction products (L1T), downloaded from United States Geological Survey (USGS – http://glovis.usgs.gov) website. The data used in this study was grouped into two categories (Table 1): the thermal infrared data (band 10) was used to calculate temperature, the red (band 4) and near infrared band (band 5) to calculate surface emissivity based on normalized difference vegetation index (NDVI).

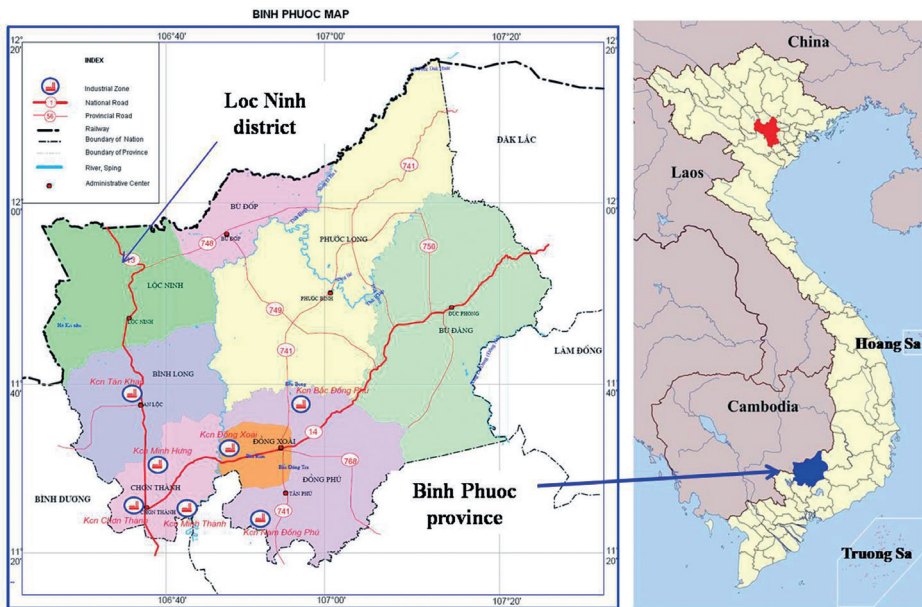The SW algorithm is based on the different atmospheric absorption behavior of two ra-

Fig. 1. The study area, Loc Ninh district, Binh Phuoc province, Vietnam

Table 1. Overview of the satellite scenes applied in this study

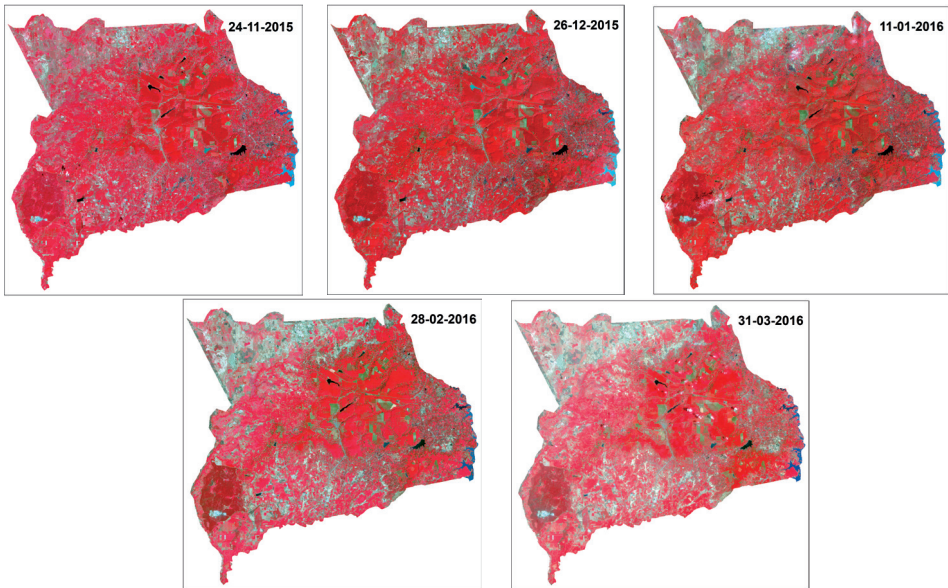| No.	Data type	Band used for temperature	Band used for NDVI	Time of data acquisition
1	LANDSAT 8	10	4, 5	24 November 2015
2	LANDSAT 8	10	4, 5	26 December 2015
3	LANDSAT 8	10	4, 5	11 January 2016
4	LANDSAT 8	10	4, 5	28 February 2016
5	LANDSAT 8	10	4, 5	31 March 2016

Fig. 2. LANDSAT 8 multispectral images in Loc Ninh district, RGB:543
Methodology

Table 2. SW coefficient values for TIRS band of Landsat 8 imagery

No.	Constants	Value
1	C_0	-0.268
2	C_1	1.378
3	C_2	0.183
4	C_3	54.300
5	C_4	-2.238
6	C_5	-129.200
7	C_6	16.400

diometric channels within the 10 – 12.5μm window region (Rongali et al. 2018). The basis of the SW algorithm is the radiance attenuation for atmospheric absorption, which is proportional to the radiance difference of simultaneous measurements at two different wavelengths, each of them being subject to varying amounts of atmospheric absorption (McMillin 1975; Rongali et al. 2018). According to this algorithm, LST can be determined by the following formula (Jiménez-Muñoz et al. 2014):
Where:

T_s – land surface temperature;
T_{B10}, T_{B11} – brightness temperature of band 10 and 11 of Landsat 8 imagery;
W – atmospheric water vapor content (g/cm²). The value of atmospheric water vapor content is calculated using formula proposed by Huazhong (Huazhong et al. 2014);
ε – mean emissivity;
$\Delta\varepsilon$ – emissivity difference;
C_0 to C_6 – SW coefficients values. The values of SW coefficients are given in Table 2 (Sobrino et al. 2006; Skokovic et al. 2014).

The flowchart of SW algorithm utilized in the present study for the estimation of LST is shown in Fig. 3.
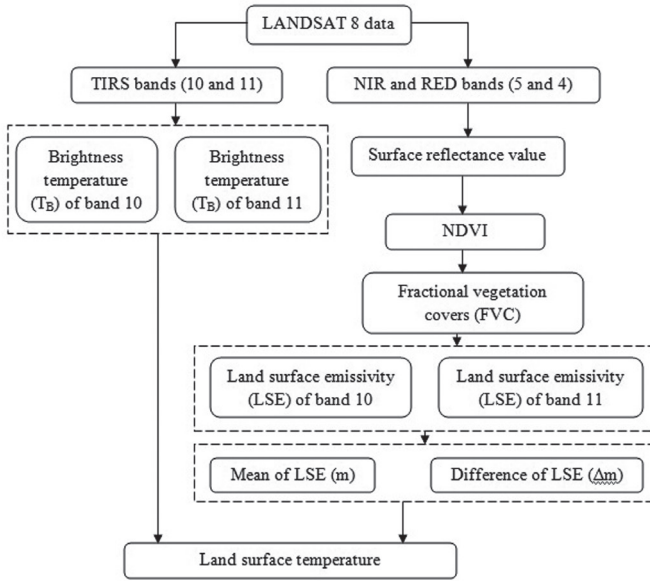
$$T_s = T_{B10} + c_1(T_{B10} - T_{B11}) + c_2(T_{B10} - T_{B11})^2 + ... \atop ... + c_0 + (c_3 + c_4 w)(1 - \varepsilon) + (c_5 + c_6 w)\Delta\varepsilon \quad (1)$$

Quang Khanh Nguyen, Le Hung Trinh et al.   LAND SURFACE TEMPERATURE DYNAMICS ...

79 GES 01|2019

Fig. 3. Split-Window algorithm for LST retrieval

In first step, OLI and TIRS band data must be converted to TOA spectral radiance using the radiance rescaling factors provided in the metadata file (Landsat.usgs.gov, 2018):

$$L_\lambda = M_L \cdot Q_{cal} + A_L \qquad (2)$$

where:

L_λ - TOA spectral radiance (Watts/(m^2 * srad * μm)),

M_L - Band-specific multiplicative rescaling factor from the metadata (RADIANCE_MULT_BAND_x, where x is the band number) (Landsat.usgs.gov, 2018),

A_L - Band-specific additive rescaling factor from the metadata (RADIANCE_ADD_BAND_x, where x is the band number) (Landsat.usgs.gov, 2018),

Q_{cal} - Quantized and calibrated standard product pixel values (DN).

Table 3. LANDSAT 8 TIRS spectral radiance ML, AL dynamic ranges

No.	Data type	Band	M_L	A_L
1	LANDSAT 8 TIRS	10	3.3420×10^{-4}	0.10000

In second step, the LANDSAT thermal band data (band 10 and band 11) can be converted form spectral radiance to brightness temperature using following equation (Landsat.usgs.gov, 2018):

$$T_B = \frac{K_2}{In(\frac{K_1}{L_\lambda}+1)} \qquad (3)$$

where:

T_B – At satellite brightness temperature (K),
K_1 – Calibration constant 1 (W/(m^2.sr.μm)),
K_2 – Calibration constant 2 (K) (Landsat.usgs.gov, 2018).

For determining LST from LANDSAT data, values of land surface emissivity are needed. In this paper, the surface emissivity is

Table 4. LANDSAT 8 thermal band calibration constants

No.	Data type	Band	K_1 (W/(m^2.sr.μm))	K_2 (Kelvin)
1	LANDSAT 8	10	774.89	1321.08
2	LANDSAT 8	11	480.89	1201.14

determined by using method based on NDVI image, which proposed by Valor and Caselles (1996) by following equation (Valor and Caselles 1996):

$$\varepsilon = \varepsilon_v \cdot P_v + \varepsilon_s (1 - P_v) \qquad (4)$$

where:

ε – Surface emissivity,

ε_v, ε^s – Emissivity of pure vegetation covers and pure soil areas, respectively.

P_v - The percentage of vegetation in one pixel, which calculated by equation (Vlassova et al. 2014):

$$Pc = \left(\frac{NDVI - NDVI_{soil}}{NDVI_{veg} - NDVI_{soil}} \right)^2 \qquad (5)$$

where:

NDVI – normalized difference vegetation index, which can be calculated by equation (Rouse et al. 1973):

$$NDVI = \frac{NIR - RED}{NIR + RED} \qquad (6)$$

RED and NIR – the spectral reflectance in red and near – infrared band, respectively. NDVIveg. and NDVIsoil - the NDVI values of vegetation and open soil, which are determined experimentally using a series of test area for vegetation and open soil.

For calculating NDVI index, the digital number of red and near infrared band was converted to surface reflectance value. In this study, one very advance atmospheric approach (FLAASH) has been applied on the Landsat 8 multispectral image, and then, the NDVI is calculated according to Eq. 7.

The land surface emissivity images of bands 10 and 11 are used to calculate mean and difference emissivity:

$$\varepsilon = \frac{\varepsilon_{10} + \varepsilon_{11}}{2} \qquad (7)$$

$$\Delta\varepsilon = \varepsilon_{10} - \varepsilon_{11} \qquad (8)$$

In last step, LST can be calculated by following equation (1).

RESULTS AND DISCUSSION

The reflectance values for red and near infrared channels of LANDSAT 8 data was used to calculate normalized difference vegetation index (NDVI). For determining surface emissivity by this methodology, values of soil and vegetation emissivity are needed. The emissivities of pure soil and pure vegetation cover were calculated from the MODIS UCSB emissivity library using method proposed by Tang (Tang et al. 2011). Soil and vegetation emissivities for Landsat 8 TIRS bands are listed in Table 5 (Yu et al. 2014).

Basing on the emissivities values of soil and vegetation, emissivity image was prepared using method of Valor and Caselles by using formula (5).

From brightness temperature and land surface emissivity images, the LST image was obtained by using Spatial Modeler of ERDAS Imagine 2014 program. Fig. 4 shows the spatial distribution of LST in Loc Ninh district, Binh Phuoc province (Southeast region of Vietnam) in dry season 2015 – 2016.

The LST ranged from 296.85 to 316.04 K in November 24, 2015; 292.52 to 311.17 K in December 26, 2015; 298.85 to 313.92 K in January 11, 2016; 298.42 to 321.27 K in February 28, 2016 and 300.20 to 321.53 K in March 31, 2016. Thus, it can be seen that the minimum and maximum LST in the early months of the dry season 2015 – 2016 (November and December) is much lower than in February and March (the end of dry season). The average LST in dry season 2015 – 2016 in Loc Ninh district, Binh Phuoc province also increased significantly, corresponding to 301.02 K in

Table 5. Emissivities of soil and vegetation for Landsat 8 TIRS band 10 and 11

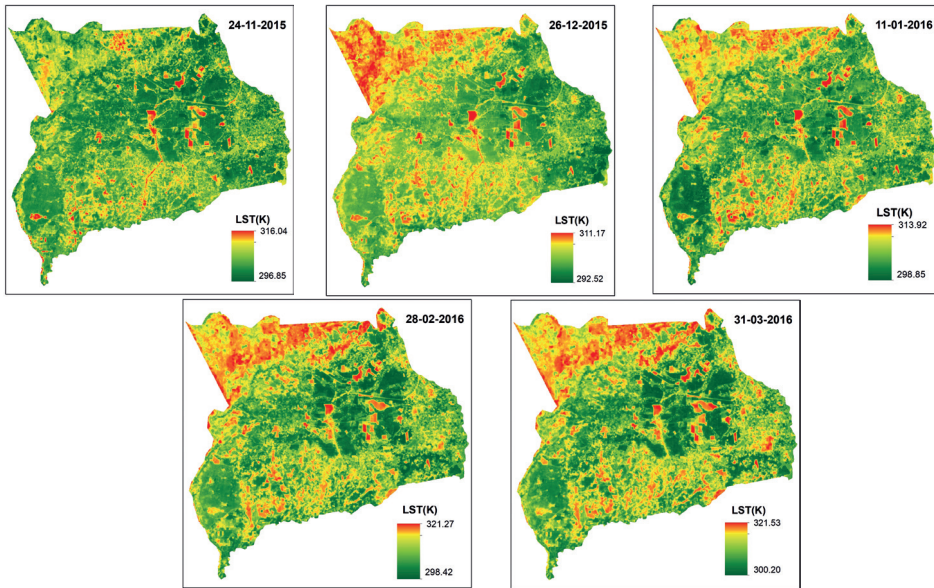| No.	Band	Soil	Vegetation
1	Band 10	0.9668	0.9863
2	Band 11	0.9747	0.9896

Fig. 4. LST over study area in dry season 2015 – 2016 retrieval from LANDSAT 8 data

November 24, 2015; 300.89 K in December 26, 2015; 303.82 K January 11, 2016; 305.18 K in February 28, 2016 and 308.42 K in March 31, 2016. According to obtained result, the northern area has highest LST in all months of dry season 2015 – 2016 (Fig. 4). These areas have sparse vegetation cover and uncultivable land. High LST are also recorded in agricultural land use and residential land in the center and southern part of the study area. Meanwhile the area with full vegetation coverage in center of study area has much lower LST.

LST data from 10 measurements points at February 28, 2016 (Fig. 5d) were used in the comparison with temperature calculated from Landsat 8 image, which acquired from same day. This in situ data were observed in the framework of the ministry-level project (Ministry of Natural Resources and Environment (Vietnam), No. 2015.08.10) and were collected from 10:00 am to 11:00 am local time in the day selected. Comparison between the LST at the measurement points and the results calculated from the Landsat 8 satellite image (February 28, 2016) based on SW and MW algorithms is presented in Table 6. It can be seen that LST at the measurements points is lower than the temperature calculated from the Landsat 8 image. The

biggest difference between in situ data and LST calculated from the Landsat 8 image is 1,75 (K) degree. In addition, it can be seen that the LST value determined by SW and single-channel (SC) algorithms are highly similar. However, overall the LST value determined by used SW algorithm tends to be smaller than using the SC algorithm (Table 6). Thus, the difference between the LST values determined by used SW algorithm and the in situ data is lower than using the SC algorithm.

The LST distribution map of the study area displays the different zone of temperatures. The density sliced image shows seven temperature zones that represents greater than 310, 309 – 310, 307 – 309, 305 – 307, 303 – 305, 301 – 303 and less than 301 K respectively. LST distribution maps in Loc Ninh district, Binh Phuoc province in dry season 2015 – 2016 are shown in Fig. 4 and Table 7. Analysis of the results showed that, in the early of dry season, much of the study area has a lower LST (less than 301 K), corresponding to 57,12% and 58,11% of the total area on November 24 and December 26, 2015. Areas with temperatures between 301 and 303 K also occupy significant areas in the early dry season (33,57% and 22.20% of the total area on November 24 and December 26,

Table 6. Compare the LST at the measurement points and the results calculated from the Landsat 8 satellite image

No. of monitoring location	Coordinates	LST (K)			Difference (K)
		From remote sensing data		In situ data	
		SW algorithm	SC algorithm (band 10)		
1	11° 49'24" N	308.45	309.31	307.50	0.95
	106° 35'48" E				
2	11° 50'59" N	310.34	310.45	309.10	1.24
	106° 35'27" E				
3	11° 50'24" N	311.27	311.94	310.20	1.07
	106° 31'20" E				
4	11° 51'14" N	302.68	302.93	301.40	1.28
	106° 36'07" E				
5	11° 50'49" N	310.65	310.80	308.90	1.75
	106° 35'36" E				
6	11° 50'28" N	309.29	309.48	308.30	0.99
	106° 34'47" E				
7	11° 51'24" N	300.78	300.90	299.50	1.28
	106° 36'17" E				
8	11° 51'34" N	300.47	300.75	299.20	1.27
	106° 35'57" E				
9	11° 50'26" N	303.88	303.97	303.10	0.78
	106° 36'07" E				
10	11° 52'10" N	313.74	313.81	312.50	1.24
	106° 39'16" N				

2015). Areas with LST over 309 K occupy relatively small areas; especially areas with temperatures above 309 K are almost negligible (less than 0.1% of the total study area at the early of dry season).

Areas with LST less than 301 K strongly decreased at the mid-dry season (January 2016), which occupies only 5,41% of the total area of the district. Most of the study area at the mid-dry season has LST between 301 to 307 K (over 92% of the total area). Areas with LST over 307 K, although increased compared to the early of dry season, however, it accounts for over 2% of the total study area.

The LST increases rapidly at the end of the dry season, from the end of February 2016. Most of the study area at the end of dry season 2015 – 2016 has LST over 303 K, in that area with LST over 309 K a significant

increase, corresponding to 20,46% and 31,20% of the total study area on February 28 and March 31, 2016. Thus, it can be noticed, LST of Loc Ninh district tend to increase significantly in dry season 2015 – 2016, in that March is considered to be the hottest month. This is also consistent

with monitoring data at meteorological stations and in situ data of ministry-level project (Ministry of Natural Resources and Environment (Vietnam), No. 2015.08.10).
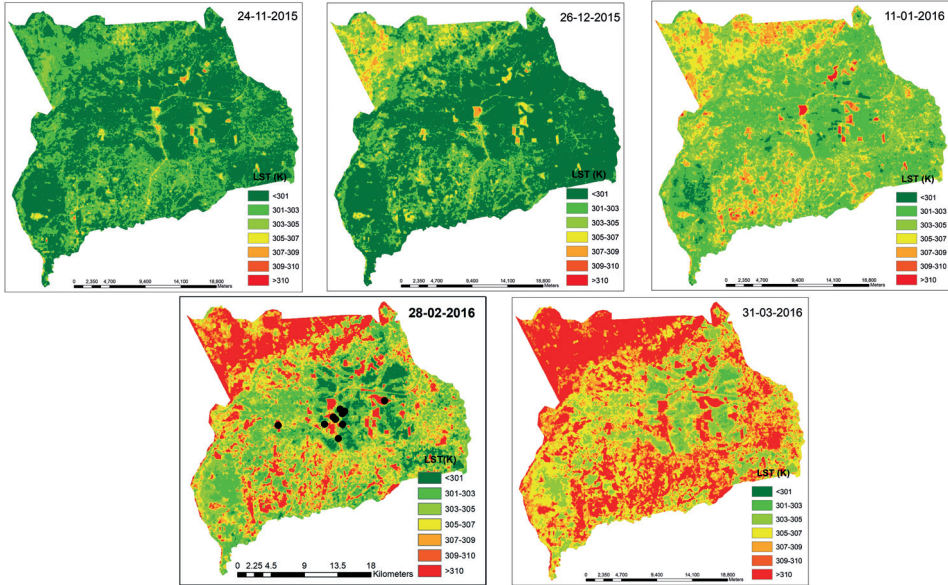

Fig. 5. Spatial distribution of LST over study area in dry season 2015 – 2016 using LANDSAT 8 data

Table 7. Temporal dynamics of LST in Loc Ninh district, Binh Phuoc province in dry season 2015 - 2016

No.	LST (K)	Area									
		November 24, 2015		December 26, 2015		January 11, 2016		February 28, 2016		March 31, 2016	
		ha	%	ha	%	ha	%	ha	%	ha	%
1	< 301	48580.56	57.12	49422.56	58.11	4601.21	5.41	5162.54	6.07	2423.93	2.85
2	301-303	28551.29	33.57	18881.1	22.2	30796.61	36.21	16780.37	19.73	13837.64	16.27
3	303-305	6259.68	7.36	10112.44	11.89	25276.86	29.72	19714.59	23.18	17988.08	21.15
4	305-307	1292.76	1.52	5307.12	6.24	15972.39	18.78	16559.24	19.47	17350.2	20.4
5	307-309	314.685	0.37	1233.23	1.45	6693.44	7.87	9432.05	11.09	6914.57	8.13
6	309-310	34.02	0.04	25.52	0.03	995.09	1.17	13276.31	15.61	22912.47	26.94
7	> 310	17.01	0.02	68.04	0.08	714.42	0.84	4124.93	4.85	3623.13	4.26

CONCLUSION

In this study, we applied SW algorithm to retrieve LST from Landsat 8 TIRS data for a case study of Southeast region of Vietnam in 2015 – 2016 dry season. Results obtained from the proposed SW algorithm have been compared with the results obtained from the SC algorithm (using only band 10) and in situ data of LST to assess the performance of the SW algorithm. It is observed that the LST obtained from SW and SC algorithms are having similar order of values, however, the SC algorithm estimates higher temperature values as compared with the SW algorithm.

The spatial distribution of LST obtained from SW algorithm showed that LST in Loc Ninh district, Binh Phuoc province (Southeast region of Vietnam) at the end of 2015 – 2016 dry season is a significant increase compared to the early dry sea-son. This increase expressed in minimum, maximum and average LST, especially areas with temperatures higher than 309 K. The study reveals that the central part of Loc Ninh district with high canopy cover has lower LST, whereas in the northern part with barren lands and residential area have high LST values.

The results obtained in this study can be used to map and evaluate the dynamics of LST, and to provide the input information for drought assessment and monitoring models.

ACKNOWLEDGMENTS

REFERENCES

Alipour T., Sarajian M.R., Esmaseily A. (2004). Land surface temperature estimation from thermal band of LANDSAT sensor, case study: Alashtar city. The International Archives of the Photogrammetry. Remote Sensing and Spatial Information Sciences, 38(4)/C7.

Alshaikh A.Y. (2015). Space application for drought assessment in Wadi-Dama (West Tabouk), KSA. The Egyptian Journal of Remote Sensing and Space Science, 18, 543 – 553.

Balling R.C., Brazel S.W. (1988). High – resolution surface temperature patterns in a complex urban Terrain. Photogrammetric engineering and Remote sensing, 54(9), 1289 – 1293.

Cai Q., Ki E., Jiang R. (2017). Analysis of the relationship between land surface temperature and land cover changes using multi-temporal satellite data. Nature Environment and Pollution Technology, 16(4), 1035 – 1042.

Carnahan W.H., Larson R.C. (1990). An analysis of an urban heat sink. Remote Sensing of Environment, 33(1), 65–71.

Chen J., Wang C., Jiang H., Mao L., Yu Z. (2011). Estimating soil moisture using temperature – vegetation dryness index (TVDI) in the Huang-huai-hai (HHH) plain. International Journal of Remote Sensing, 32, 1165 – 1177.

Cueto G., Jauregui Ostos E., Toudert D., Tejeda Martinez A. (2007). Detection of the urban heat island in Mexicali and its relationship with land use. Atmosfera, 20(2), 111 – 131.

Du C., Ren H., Qin Q., Meng J., Li J. (2014). Split-window algorithm for estimating land surface temperature from Landsat 8 TIRS data. International Geoscience Remote Sensing Symposium 3578–3581, https://doi.org/10.1109/IGARSS.2014.6947256

Galve J.M., Coll C., CasellesV., Valor E., Mira M. (2008). Comparison of split-window and single-chanel methods for land surface temperature retrieval from MODIS and ASTER data. International Geoscience Remote Sensing Symposium 3:294 – 297, https://doi.org/10.1109/IGARSS.2008.4779341

Grishchenko M.Y. (2012). ETM+ thermal infrared imagery application for Moscow urban heat island study. Current Problems in Remote Sensing of the Earth from Space, 9(4), 95-101 (In Russian).

Jiménez-Muñoz J.C, Sobrino J.A., Skoković D., Mattar C., Cristóbal J. (2014). LST retrieval methods from Landsat-8 thermal infrared sensor data. IEEE Geoscience and Remote Sensing Letters, Vol. 11, No. 10, 1840-1843, doi: 10.1109/LGRS.2014.2312032.

Julien Y., Sobrino J.A. (2009). The yearly land cover dynamics method: an analysis of global vegetation from NDVI and LST parameters. Remote Sensing of Environment, 113, 329 – 334.

Kumar K.S., Bhaskar P.U., Padmakumari K. (2012). Estimation of land surface temperature to study urban heat island effect using LANDSAT ETM+ image. International journal of Engineering Science and technology, 4(2), 771 – 778.

Huazhong R., Du C., Qin Q., Liu R. (2014). Atmospheric water vapor retrieval from Landsat 8 and its validation, IEEE International Geoscience and Remote Sensing Symposium, 3045 – 3048, doi: 10.1109/IGARSS.2014.6947119.

Hyung Moo Kim, Beob Kyun Kim, Kang Soo You (2005). A statistic correlation analysis algorithm between land surface temperature and vegetation index. International Journal of Information Processing Systems, 1(1), 102 – 106.

Lambin T.R., Ehrlich D. (1996). The surface temperature – vegetation index space for land cover and land cover change analysis. International Journal of Remote Sensing, 17(3), 163 – 187.

Landsat.usgs.gov, (2018). Landsat 8 (L8) data users handbook, Version 3.0. [online] Available at http://landsat.usgs.gov [Accessed 31 October 2018]

Li S., Jiang G. (2018). Land surface temperature retrieval from Landsat-8 data with the ggeneralized split-window aalgorithm. IEEE Access, Vol. 6, 18149-18162, doi: 10.1109/ACCESS.2018.2818741.

Lo C.P., Quattochi D.A., Luvall J.C. (1997). Application of high resolution thermal infrared remote sensing and GIS to assess the urban heat island effect. International Journal of Remote Sensing, 18, 287 – 304.

Locninh.binhphuoc.gov.vn, (2018). Locninh district Official Website. [online] Available at http://locninh.binhphuoc.gov.vn [Accessed 20 October 2018]

Mallick J., Kant Y., Bharath B.D. (2008). Estimation of land surface temperature over Delhi using LANDSAT 7 ETM+. Geophysics Union, 3, 131 – 140.

Marchukov V.S., Trinh L.H. (2013). Monitoring land surface temperature using LANDSAT thermal infrared image. Izvestiya Vuzov «Geodesy and Aerophotography», 6, 41 – 43 (In Russian).

McMillin L. (1975). Estimation of sea surface temperatures from two infrared window measurements with different absorption. Journal of Geophysical Research 80:5113–5117,

Mira M., Valor E., Boluda R., Caselles V., Coll C. (2007). Influence of the soil moisture effect on the thermal infrared emissivity. Tethes, 4, 3 – 9, doi: m10.3369/Tethys.2007.4.01.

Parida B.R., Oinam B., Patel N.R., Sharma N., Kandwal R., Hazarika M.K. (2008). Land surface temperature variation in relation to vegetation types using MODIS satellite data in Gujarat state of India. International Journal of Remote Sensing, 29(14), 4219 – 4235.

Rongali G., Keshari A.K., Gosain A.K., Khosa R. (2018). Split-window algorithm for retrieval of land surface temperature using Landsat 8 thermal infrared data. Journal of Geovisualization and Spatial Analysis, Published online 05 September 2018, Springer, 19 pp.

Rouse J.W., Hass R.H., Schell J.A., Deering D.W. (1973). Monitoring vegetation systems in the Great Plains with ERTS. In: Earth Resources Technology Satellite-1 Symposium, 3, Washington- DC, p. 309-317

Rozenstein O., Qin Z., Derimian Y., Karnieli A. (2014). Derivation of land surface temperature for landsat-8 TIRS using a split window algorithm. Sensors 14:5768–5780, https://doi.org/10.3390/s140405768

Sandholt I., Rasmussen K., Anderson J. (2002). A simple interpretation of the surface temperature/vegetation index space for assessment of the surface moisture status. Remote Sensing of Environment, 79, 213–224.

Shang Y., Hu Q., Liu G., Zhang H. (2017). Winter wheat drought monitoring and comprehensive risk assessment: case study of Xingtai administrative district in North China, Journal of Environmental Science and Engineering, A6, 135 – 143.

Sobrino J.A., Jimenez-Munoz J.C., Zarco-Tejada P.J., Guadalupe Sepulcre-Canto, Eduardo de Miguel (2006). Land surface temperature derived from airborne hyperspectral scanner thermal infrared data. Remote Sensing of Environment, 102, 99 – 115.

Skokovic D., Sobrino J.A., Jiménez Muñoz J.C., Soria G., Julien Y., Mattar C., Cristóbal J. (2014). Calibration and validation of land surface temperature for Landsat8- TIRS sensor TIRS Landsat-8 characteristics. Land Product Validation and Evolution ESA/ESRIN 27.

Tang B.H., Wu H., Li C., Li Z.H. (2011). Estimation of broadband surface emissivity from narrowband emissivities. Optical Express, 19, 185 – 192.

Thakur P., Gosavi V. (2018). Estimation of temporal land surface temperature using thermal remote sensing of Landsat 8 (OLI) and Landsat 7 (ETM+): A case study in Sainj river basin, Himachal Pradesh, India. Environment & We: International Journal of Science & Technology, Vol. 13, 29 – 45.

Tran T.V., Hoang T.L., Le V.T. (2009). Thermal remote sensing method in sudy on urban surface temperature distribution. Vietnam Journal of Earth Sciences, 31(2), 168 – 177.

Trinh L.H. (2014). Studies of land surface temperature distribution using LANDSAT multispectral image. Vietnam Journal of Earth Sciences, 36(1), 82 – 89.

Ulivieri C., Castronuovo M., Francioni R., Cardillo A. (1994). A split window algorithm for estimating land surface temperature from satellites. Advanced Space Research 14:59–65, https://doi.org/10.1016/0273-1177(94)90193-7

Valor E., Caselles V. (1996). Mapping land surface emissivity from NDVI. Application to European African and South American areas. Remote Sensing of Environment, 57, 167 – 184.

Van de Griend A.A., Owen M. (1993). On the relationship between thermal emissivity and the normalized difference vegetation index for natural surface. International Journal of Remote Sensing, 14, 1119 – 1131.

Vietnam assessment report on climate change (VARCC) (2009), Institute of strategy and policy on natural resources and environment. Hanoi, 127 pp.

Vlassova L., Perez-Cabello F., Nieto H., Martin P., Riaflo D., de la Riva J. (2014). Assessment of methods for land surface temperature retrieval from Landsat 5 TM images applicable to multiscale tree-grass ecosystem modeling, Remote Sensing, 6, 4345-4368; doi:10.3390/rs6054345.

Yu X., Guo X., Wu X. (2014). Land surface temperature retrieval from Landsat 8 TIRS – Comparison between radiative transfer equation based method, split window algorithm and single channel method, Remote Sensing, 6, 9829 – 9852, doi:10.3390/rs6109829.

Zverev A.T., Trinh L.H. (2015). Monitoring soil moisture using LANDSAT multispectral images. Issledovanie Zemli iz Kosmosa, 6, 62 – 67 (In Russian).